Object-oriented tracking of thematic and spatial behaviors of urban heat islands

Rui Zhu[a,b], Eric Guilbert[c], Man Sing Wong[b,*]

[a] *Senseable City Laboratory, Singapore-MIT Alliance for Research and Technology, Singapore*
[b] *Department of Land Surveying and Geo-informatics, The Hong Kong Polytechnic University, Hong Kong, China*
[c] *Department of Geomatics Sciences, Laval University, Québec, Canada*

Abstract

Modeling thematic and spatial dynamic behaviors of urban heat islands (UHIs) over time is vital to understand evolution of this phenomenon to mitigate warming trend in urban areas. However, previous studies conceptualized that a UHI can only have a single life-cycle with spatial behaviors (i.e. areal changes and topological transformations). A UHI can also appear and disappear periodically several times expressed by thematic and spatial integrated behaviors, which, however, has not been established yet. Thus, this study conceptualizes each UHI as an object which has thematic and spatial behaviors simultaneously and proposes several *graphs* to depict periodic life-cycle transitions triggered by the behaviors. The model is implemented in an object-relational database, and air temperatures collected from a sufficient number of weather stations are interpolated as temperature images each hour for six weeks. Results indicate that the model cannot only track the spatial and thematic evolution of UHIs through continuous time effectively, but also reveal the periodical patterns and abnormal cases sensitively.

Keywords: Spatiotemporal data modeling; Object-oriented modeling; Urban heat islands; Database management system

1. Introduction

UHIs are a major problem in most metropolitan areas, causing many adverse effects such as public health (Ding *et al.*, 2015; Kenney *et al.*, 2014; Morabito *et al.*, 2012), security threats (Cohn and Rotton, 2000; Field, 1992; Rotton and Cohn, 2004), and increased energy consumption (Fung *et al.*, 2006; Papakostas *et al.*, 2010). It is likely to be an even more serious problem in the rapidly expanding cities given the increasing urbanization process. To investigate the adverse effects and explore the causative factors of the phenomenon, automatically tracking evolution trends of UHIs in both thematic (i.e. temperature variations) and spatial (i.e. areal changes and topological transformations) dimensions over a long time period become an urgent need.

A UHI is an environmental phenomenon such that temperatures in urban areas are higher than in surrounding rural areas. Based on this perception, a UHI is commonly conceptualized as a two-dimensional field phenomenon and defined by the difference in temperatures observed in urban areas and surrounding rural areas. Previous studies estimated land surface temperature (LST) to describe urban heat islands and analyzed its correlation with social indicators (Buyantuyev and Wu, 2010), environmental indices (Hu and Brunsell, 2015), and building impacts (Yuan and Ng, 2012; Wong and Nichol, 2013; Toparlar *et al.*, 2015; Wong *et al.*, 2016). Recent studies tend to analyze discrete pixels toward clustering them as interactive objects extracted from thermal images. For example, an object-based analysis cluster pixels of thermal infrared images as polygons of objects so that a strong correlation between spatial and thermal attributes (i.e. areal extent and LST) was revealed

*Corresponding author
Email address: ls.charles@polyu.edu.hk (Man Sing Wong)

(Keramitsoglou *et al.*, 2011). However, tracking thematic and spatial changes of UHIs simultaneously over a long time period and describing the overall evolutionary trends are still challenging even though some empirical investigations have been conducted by analyzing spatio-temporal variation patterns of UHIs based on the interpolation of air temperatures collected from meteorological stations (Wu *et al.*, 2012; Kourtidis *et al.*, 2015). Thus, a spatio-temporal data model that can determine pixels of thermal images as UHI objects and track the changes of their dynamics through continuous time is needed.

Many studies modeled geographical phenomena as field objects which have enclosed and variable boundaries determined by other properties (e.g. time and thematic properties) related with the field (Goodchild et al., 2007). Their dynamics can be represented in a hierarchical framework where a *sequence* is composed of consecutive *zones* and related together in *processes*, and *events*, observing their shape changes and spatial movements from a series of images (McIntosh and Yuan, 2005; Yuan and Hornsby, 2008). For instance, moving behaviors of each object were modeled as a set of semantic *events* such as *departure* and *arrival* and patterns were constructed from several sequences of the *events* (Hornsby and Cole, 2007). Further developed models conceptualized spatiotemporal dynamic phenomena as geo-entities in relationships and implemented data structures fitted for computations (Bothwell and Yuan, 2010; Pultar *et al.*, 2010; Li *et al.*, 2013).

The above approach can also be used to model other environmental phenomena such as UHIs. However, more complex dynamics involving a single object or several different objects shall be considered. For example, a UHI can contract, split in two parts, and disappear. Oppositely, two UHIs can expand and merge together in a single one. Claramunt and Thériault (1995) proposed a series of topological processes describing a single object behavior's as an expansion or a contraction and several objects' as splits, unions, or re-allocations. Similar models were developed such that objects disappear and reappear because of merging and splitting behaviors (Renolen, 2000; Nixon and Hornsby, 2010; Bothwell and Yuan, 2011). Del Mondo *et al.* (2013) depicted these transformations as a *graph* composed by a set of nodes and several edges connecting the nodes with certain filiation relationships.

Benefiting from the above contribution, a study proposed an object-oriented spatio-temporal framework modeling spatial behavior of UHIs (Zhu *et al.*, 2016). In the framework, a UHI experiences different *sequences*, each of which corresponds to a type of behavior. For instance, a UHI sequence can be an expansion, where the UHI grows larger, a continuation if its area remains constant, or a contraction if the area is reducing over a continuous time period. These sequences are mainly due to *temperature* variations inside the UHI as the UHI effect can get more intense, remain stable or be moderated. UHI changes can be either internal with area changes or external involving topological transformations with one or several UHIs. Nevertheless, transformations and process of areal change have been defined formally as two graphs: a zone graph $\mathcal{G}_Z = (\mathcal{Z}, \mathcal{F}_z)$ denotes a set of zones ($\mathcal{Z}$) and a set of filiations ($\mathcal{F}_z$) associated with the zones, and a sequence graph $\mathcal{G}_S = (\mathcal{S}, \mathcal{E}_s)$ represents a set of sequences ($\mathcal{S}$) that have areal changes or topological transformations ($\mathcal{E}_s$).

However, the above framework cannot track thematic changes of a UHI, which is also vital to clarify evolutionary trends of the temperatures since they determine the spatial extent directly and influences its spatial behaviors as a consequence (Bothwell and Yuan, 2012). For example, an increase of the UHI temperature may lead to the expansion of its spatial extent during the nighttime but contracting during the daytime. Different mechanisms can be explored with a correlation analysis between two types of behaviors. As an object, a UHI may appear, disappear and reappear over time, having periodical process of state transitions between existence and non-existence (Hornsby and Egenhofer, 2000). The periodicity links a series of existences as a continuous process, which can extend life spans of UHIs from a few hours to a couple of days. Therefore, establishing the periodicity would be much helpful for investigation over long time periods. Moreover, tracking capability of the above framework

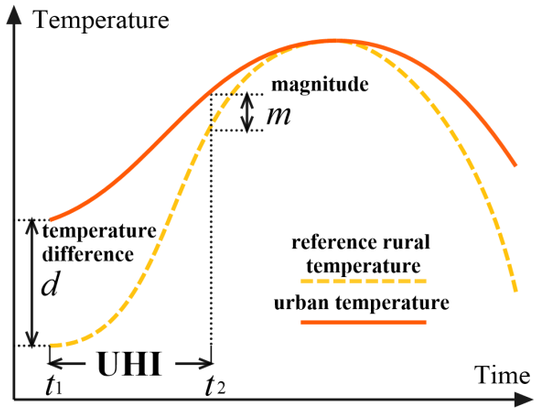

Figure 1: A UHI is with at least m degrees Celsius higher than the reference rural temperature.

can be enhanced in two aspects. First, it simply conceptualized a UHI as a homogeneous zone where temperature variations in the zone were not differentiated and thus could not be investigated. Second, it only considered *unidirectional* relationship of zones in the previous time instant to the zones in the current time, which can cause a problem that two zones having no significant overlapping with each other are still determined as associated zones unconfidently.

In summary, this study argues that previously developed models for UHIs were incomplete and should be improved. This study will: (i) define a UHI as an object in considering of temperature difference between urban and rural temperatures, (ii) model thematic behaviors of UHIs systematically, (iii) refine spatial behaviors of UHIs more logically and reliably by considering bidirectional relationship between zones, and (iv) explore new knowledges through the tracking of two types of behaviors.

2. Conceptual and logical modeling

2.1. UHI as field objects

A UHI was commonly defined as a two-dimensional field object that its temperatures were equal or higher than a reference rural temperature (Zhu *et al.*, 2016). Spatial variations of temperatures in the UHI extent were not able to be analyzed since the field was recorded as a homogeneous polygon. However, temperature distribution within the extent can vary significantly, which is worthy of being investigated. For example, a small area within a UHI extent constantly maintaining a steady and high temperature can correspond to a place with constant heat source of air conditioning. The UHI may contain several small UHIs if such small areas are also viewed as UHIs having higher intensity. To better investigate this phenomenon at different thematic intensities, a new definition of UHI is thus introduced.

Thematic and spatial properties of a geographical phenomenon can change simultaneously over time. For the UHI phenomenon, temperature changes (i.e. the thematic property) lead to extent changes (i.e. the spatial property) instantly. A UHI can be at least with certain degree Celsius higher than the reference rural temperature for formulating peaks of the temperature. This may create inclusions between UHIs when they are with a set of temperatures higher than the reference rural temperature. As shown in Figure 1, a UHI exists during t_1 and t_2 since temperature difference (d) between urban temperature and the reference rural temperature are equal or higher than a given degrees Celsius (i.e. a *magnitude*). Thereby, a UHI can have four properties, i.e., *time* (t) to provide a temporal dimension for the description of thematic and spatial evolutions, a *magnitude* (m) to represent the significance, a *zone* (z) to depict a variable extent, and an *intensity* (s) to summarize all the temperature differences in the zone at t. As a two-dimensional field, the zone of a UHI may

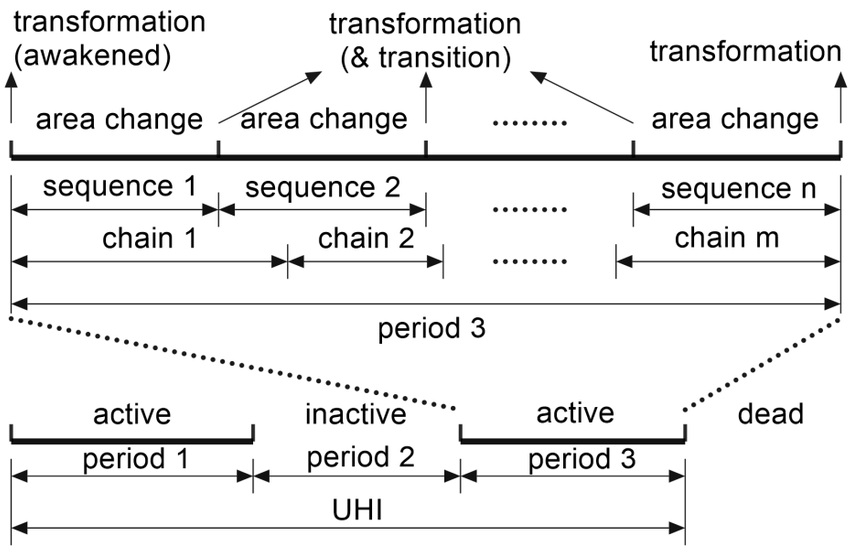

Figure 2: Complete life-cycle of a UHI. An active period contains a series of sequences and chains over a period, in which a sequence is made by a type of spatial behavior associated with transformations and chains correspond to thematic changes.

expand, contract, or remain stable possibly because the intensity grows up, drops down, or keeps constant over time.

2.2. UHI as periodical objects

UHIs periodically appeared at the same place were viewed as a series of different objects having no relationships so that each UHI could be tracked only for a few hours usually (Zhu *et al.*, 2016). This makes it difficult to investigate this phenomenon over long time period. As an object, a UHI can appear, disappear, and reappear periodically for several consecutive days, which would be much helpful for revealing thematic and spatial evolutionary trends of UHIs over a longer temporal domain (e.g., in months, seasons, or even years), by extending life span of UHIs. In this regard, life span of a UHI can extend from a single life-cycle to several *active* and *inactive* periods that connect with each other. Thereby, a UHI can have *active* and *inactive* states in its life-cycle or be *dead* if it disappears forever, and time span of each state (either *active* or *inactive*) can be named as a *period* (Figure 2). In this scenario, *appearance* of a UHI indicates a special process of *awakened* given the condition that it was *active* before.

According to the proposed spatial behaviors (Zhu *et al.*, 2016), an *active period* can start from *appearance*, *splitting*, *merging*, and *separation* for zones which are newly generated and terminate at *disappearance*, *splitting*, *merging*, and *annexation* for zones which are destroyed. However, termination of an *active period* followed by an *inactive period* indicates that the UHI temporarily disappeared and it will appear again as *awakened* in the near future. Therefore, this process requires some topological criteria:

- the temporarily disappeared zones are not caused by the absorption (*annexation* and *merging*) since the absorption makes zones destroy forever; and
- the reappeared zones do not benefit from the dispersion (*separation* and *splitting*) because the dispersion generates new objects.

Thus, only the consecutive *disappearance* and *appearance* can lead to a *awakened*, and difference between *birth* and *awakened* can be achieved by a backward searching whether there was a disappeared zone that can associate with the appeared zone. As such, a UHI can be periodical with two periods connecting with each other:

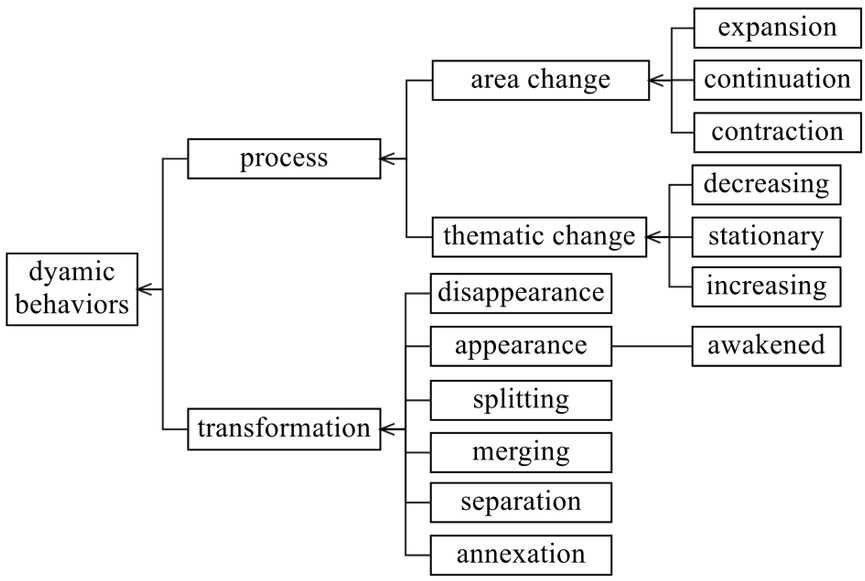

Figure 3: A hierarchical set of dynamic behaviors of UHIs.

- the *active period* is a time period that a UHI starts from appearance and ends with disappearance so that it contains a series of sequences; and
- the *inactive period* is a time period that a UHI begins with disappearance and terminates at appearance so that it contains an *empty* sequence.

2.3. Graph-based modeling of thematic behaviors

To have a more distinct and structured description, changes of the properties can be viewed as dynamic behaviors of a UHI and are thereby summarized as a set of concepts hierarchically represented in Figure 3. The figure shows that *dynamic behaviors* contains *process* that each behavior continues for a time period and *transformation* that topological changes occur at a time instant associated with two or several *processes*. Since spatial behaviors have already been discussed (Zhu *et al.*, 2016), this section focuses on the modeling of the thematic behaviors.

There could be a set of temperature differences ($D^i = \{d^i\}$) in a zone at at an instant of time t_i since temperatures in the zone can vary differently. Therefore, the intensity of a UHI u_n at t_i would be $s^i = f(D^i)$ ($s^i \geqslant m$), where s^i can be the maximum, minimum, mean or mode value of D^i. For instance, the maximum temperature could reveal the most intense character of UHIs while the mode temperature can be quantitatively representative. To maintain the unity and continuity of the thematic character, only one type of the e_c^i will be used constantly during the whole life span of a UHI. Hence, intensity relationships between zones can be represented as three qualitative descriptions: (i) *increasing* when s^i is higher than s^{i-1}; (ii) *stationary* when s^i is the same as s^{i-1}; and (iii) *decreasing* when s^i is lower than s^{i-1}.

Let a *chain* contain a series of intensities over a time period $[t_i, t_j]$ so that all the intensities of a series of zones belong to the same u_n and they have the same type of thematic filiation. Hence, a *chain* can be denoted as $a_n = \{s_n^i, \ldots, s_n^j\}$ which satisfies that both (s_n^{k-1}, s_n^k) and (s_n^i, s_n^{i+1}) correspond to the same behavior, for $\forall k \in (i+1, j]$. Thus, a new graph for all the chains can be refined: $\mathcal{G}_C = (\mathcal{A}, \mathcal{F}_c)$ where $\mathcal{A}$ is a complete set of the chains and $\mathcal{F}_c$ denotes thematic filiations when changes happen between chains. Let $\mathcal{F}_c = \mathcal{C}_c \cup \mathcal{T}_c$ such that $(s_n^{k-1}, s_n^k) \in \mathcal{C}_c$ occurs in the same UHI to represent the qualitative descriptions of the intensities, and $(s_n^{k-1}, s_m^k) \in \mathcal{T}_c$ when several UHIs are associated.

Since *intensity* is the core property that determines the existence of a UHI, chains would continue when it is *active* constantly. Thus, $\mathcal{C}_c$ distribution along with the temporal domain can depict thematic behaviors of a UHI. Let a_n^{ij-1}, a_n^{ij}, and a_n^{ij+1} denote three consecutive chains of u_n, the two edges

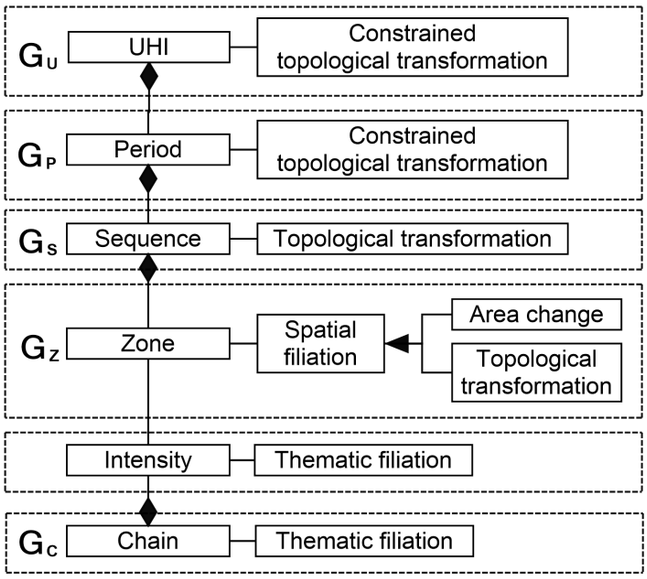

Figure 4: Five hierarchical graphs for UHIs.

$(a_n^{i_j-1}, a_n^{i_j})$ and $(a_n^{i_j}, a_n^{i_j+1})$ can be stated as the following:

- if $a_n^{i_j-1}$ increases and $a_n^{i_j}$ decreases, u_n reaches a *peak* at the transition;
- if $a_n^{i_j-1}$ decreases and $a_n^{i_j}$ increases, u_n reaches a *low* at the transition;
- if $a_n^{i_j-1}$, $a_n^{i_j}$, and $a_n^{i_j+1}$ respectively increases, stays stationary and decreases, chain $a_n^{i_j}$ corresponds to a plateau. u_n is *reaching a plateau* and *leaving a plateau* during the transitions;
- if $a_n^{i_j-1}$ decreases, $a_n^{i_j}$ keeps stationary, and $a_n^{i_j+1}$ increases, chain $a_n^{i_j}$ is as a floor. u_n is *reaching a floor* and *leaving a floor* during the transitions; and
- if both $a_n^{i_j-1}$ and $a_n^{i_j+1}$ increase or decrease and $s_n^{i_j}$ is stationary, chain $a_n^{i_j}$ leads to a pause for the thematic evolution. The two consecutive transitions are *stabilization* and *resumption*.

2.4. Graph-based modeling of periods

An *active period* contains a series of sequences denoted as $p_n^a = \{q_n^c, \ldots, q_n^d\}$. For zones in each sequence over a temporal domain $[t_i, t_j]$, they may have either areal changes or transformations belonging to the same u_n, where $\forall k, i < k \leq j, (z_n^{k-1}, z_n^k) = (z_n^i, z_n^{i+1}) \in \mathcal{F}_z$. Similarly, an *inactive period* contains an empty sequence and is denoted as p_n^b so that a *awakened* connects with an empty sequence and generates another practical sequence. Thereby, all the periods can be refined into a graph $\mathcal{G}_P = (\mathcal{P}, \mathcal{E}_p)$ where $\mathcal{P}$ is the set of nodes denoting periods and $\mathcal{E}_p$ is the set of edges representing the state transitions between the periods. More specifically, the edges can be characterized by the transformations they are associated with. When several UHIs have interactive evolution in the same urban area or spatial contiguous city clusters, a graph can be introduced as $\mathcal{G}_U = (\mathcal{U}, \mathcal{E}_u)$, where $\mathcal{U}$ is a set of UHIs that makes the graph nodes and $\mathcal{E}_u$ is the edges composed by topological transformations which lead the creation and destruction of the UHIs.

In summary, three new graphs have been proposed at this stage together with another two, i.e., the zone-graph $\mathcal{G}_Z$ and the sequence-graph $\mathcal{G}_S$ (Zhu *et al.*, 2016). The five graphs are presented hierarchically in Figure 4, which draws a complete description of thematic and spatial behaviors of UHIs. Thematic filiations construct the chain-graph $\mathcal{G}_C$. Relying on the intensities, $\mathcal{G}_Z$ describes the most elementary spatial-evolution and builds the foundation of $\mathcal{G}_S$ so that spatial revolution pattern associated with topological transformations starts to be revealed. Benefiting from $\mathcal{G}_S$, $\mathcal{G}_P$ records complete life-cycle of a UHI which may have several consecutive sequences associated with some particular transformations such that all of the UHIs evolution can be finally tracked in $\mathcal{G}_U$.

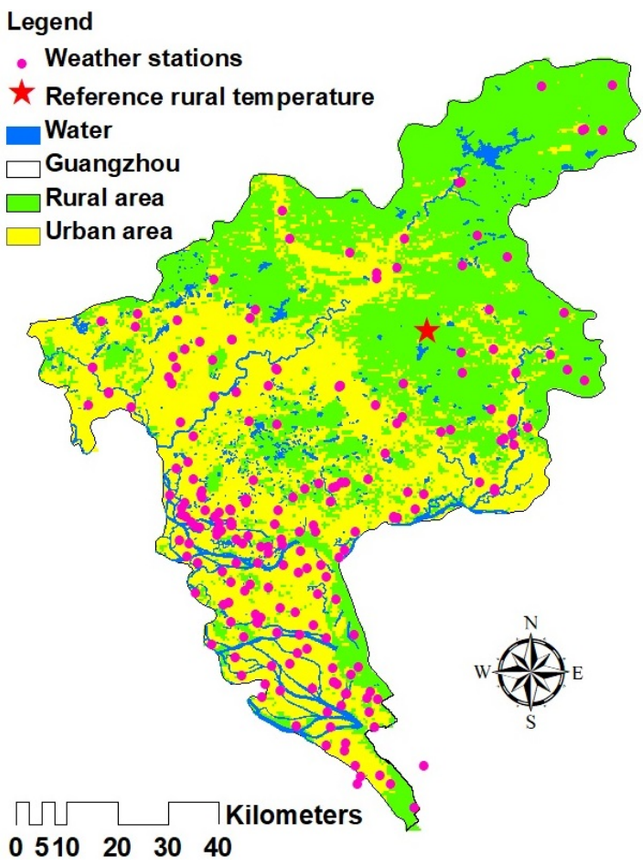

Figure 5: Weather stations are dominantly located in the urban areas of Guangzhou.

3. Application of UHI tracking

3.1. Study area and preprocessing

Guangzhou was selected as the study area to test the effectiveness of the model. The model requires high temporal resolution of the data set to track changes of UHIs continuously. Thus, hourly updated near-surface (approximately 1.5 meters above the land surface) air temperatures were acquired from 216 automatic weather stations. To analyse evolutionary trends of UHIs over a long time, data were collected for six weeks in year 2015 with an interval of 21 days between every two weeks, from July 31 to August 6, August 28 to September 3, September 25 to October 1, October 23 to October 29, November 20 to November 26, and December 18 to December 24. Most of the weather stations are located in the urban areas as shown in Figure 5.

This study used Universal Kriging for interpolating the images since the method can highlight hotspot regions of UHIs supposing the input data set contains an overriding trend (Chai *et al.*, 2011; Hofstra *et al.*, 2008; Irmak *et al.*, 2010; Stahl *et al.*, 2006). Since weekly-averaged root mean square errors of the six sequential weeks were 1.06 °C, 0.99 °C, 1.13 °C, 1.06 °C, 1.07 °C, and 1.03 °C, the magnitude m should be notably larger than 1 °C to extract zones of UHIs confidently. Temperatures observed at the red star symbol in Figure 5 were located in the Dajinfeng Eco-scenic Park, which is a large forestry area close to urban areas. Therefore, the temperatures were used as the reference rural temperatures to extract zones of UHIs.

3.2. Extraction of UHI changes

The history of each UHI was built by studying overlapping zones at consecutive time instants. We consider here that if two zones share a similar position, they are most likely belonging to the same UHI. Our previous approach only considered the relation between the intersection $z^i \cap z^{i-1}$ and z^{i-1} where z^i and z^{i-1} are two zones at consecutive time instants t_{i-1} and t_i (Zhu *et al.*, 2016). Since

UHIs remain located around the same location and do not have significant displacements, it is more convincing if related zones have a significant intersection $z^i \cap z^{i-1}$ for both z^i and z^{i-1}.

Given two zones z and z', we consider that z significantly overlaps z' and we note it $SO(z, z')$ if both zones overlap and the area of their intersection is large with regard to the area of z'. If we note $0 < \varepsilon < \frac{1}{2}$ a constant, significant overlap is defined by:

$$SO(z, z') \Leftrightarrow \frac{\text{area}(z \cap z')}{\text{area}(z')} > 1 - \varepsilon \tag{1}$$

Fixing $\varepsilon < \frac{1}{2}$ guaranties that for a given zone z', it is not possible to find two disjoint zones significantly overlapping z'. This relation is not symmetric and the relation $SO(z', z)$ may be false, for example if z is much larger than z'. If both relations are true, both zones significantly overlap and we note this relation $OO(z, z')$.

$$OO(z, z') \Leftrightarrow SO(z, z') \wedge SO(z', z) \tag{2}$$

Although a zone cannot be significantly overlapped by two disjoint zones, it can significantly overlap several zones. For a given set of zones Z, the set of all zones significantly overlapped by z is given by

$$S_Z(z) = \{SO(z, z') | z' \in Z\} \tag{3}$$

For a given zone z, the number of zones in $S_Z(z)$ is given by $\#S_Z(z)$. If Z is the set of all zones $\mathcal{Z}_i$ at time i, we simply note $S_{\mathcal{Z}_i}$ as S^i and its cardinality $\#S^i$. As zones at a given time instant are supposed to be disjoint, we have

$$z \in \mathcal{Z}_i, z' \in \mathcal{Z}_i \Rightarrow z \cap z' = \varnothing \tag{4}$$

$$z_1^i \in \mathcal{Z}_i, z_2^i \in \mathcal{Z}_i, z^j \in \mathcal{Z}_j \Rightarrow \neg \left(SO(z_1^i, z^j) \wedge SO(z_2^i, z^j) \right) \tag{5}$$

Obviously, the type of spatial behavior of a UHI can be determined by (i) the number of zones it is associated with, and (ii) the type of filiation with these zones. The UHI has areal change if it associates with only one zone and without any topological transformations. If no overlapping or no association occurs, this UHI appears or disappears. Otherwise, it can have transformations when overlapping and associating with several other zones. Thus, changes for zones at t_i are further refined:

- *appearance*: u_n appears at t_i if there is no significant overlap between a zone z_i and any zones at t_{i-1};
- *disappearance*: u_n disappears at t_i if there is no significant overlap between a zone z_i and any zones at t_{i+1};
- *expansion*: one zone at t_{i+1} significantly overlaps one zone at t_i;
- *continuation*: two zones at t_{i-1} at t_i significantly overlap and their areas are equivalent;
- *contraction*: one zone at t_{i-1} significantly overlaps one zone at t_i;
- *merge*: one zone z_i at t_i overlaps several zones at t_{i-1} and each overlapping area is significant to its corresponding zone at t_{i-1}. If only one overlapping area is exclusively significant to the zone at t_i, the associated zone at t_{i-1} continues as the zone at t_i and an *annexation* happens. If all the overlapping areas are insignificant to the zone at t_i, a *merging* can be determined;
- *split*: several zones at t_i overlap one zone at t_{i-1} and each overlapping area is significant to its corresponding zone at t_i. If area of the zone at t_{i-1} equals to one particular zone at t_i, a *separation* is derived. Otherwise, a *splitting* occurs.

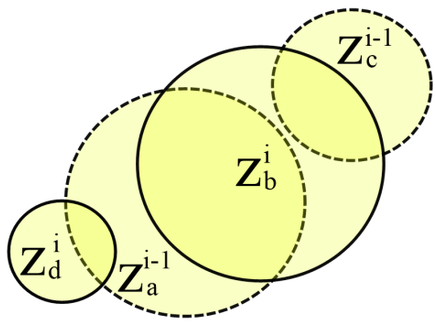

Figure 6: Different overlapping scenarios generate different spatial behaviors.

3.3. Computation

We now can redefine the transitions between zones from their relationships. If a UHI does not undergo any transformation between time t_{i-1} and time t_i, then $\#S^i(z^{i-1})$ and $\#S^{i-1}(z^i)$ cannot be greater than 1. If no change in area occurs, both zones significantly overlap such that $OO(z^{i-1}, z^i)$ is true. Hence for two zones $z^{i-1} \in \mathcal{Z}_{i-1}$ and $z^i \in \mathcal{Z}_i$, continuation is defined by

$$\text{continuation}(z^{i-1}, z^i) \Leftrightarrow OO(z^{i-1}, z^i) \wedge \#S^i(z^{i-1}) = 1 \wedge \#S^{i-1}(z^i) = 1 \tag{6}$$

In a contraction, z^{i-1} is bigger than z^i hence only $SO(z^{i-1}, z^i)$ is true. As a continuous process, no other zone is involved in the process. Therefore, the contraction is defined by

$$\text{contraction}(z^{i-1}, z^i) \Leftrightarrow SO(z^{i-1}, z^i) \wedge \#S^i(z^{i-1}) = 0 \wedge \#S^{i-1}(z^i) = 1 \tag{7}$$

Similarly, the expansion is defined by

$$\text{expansion}(z^{i-1}, z^i) \Leftrightarrow SO(z^i, z^{i-1}) \wedge \#S^i(z^{i-1}) = 1 \wedge \#S^{i-1}(z^i) = 0 \tag{8}$$

Referring to Figure 3, a process (more specifically for an area change) is a relationship involving a limited number of zones. Anything that is not a process can then be defined as a transformation. The above three relationships correspond to processes where no topological change occurs. A more general relation can be defined relating two consecutive zones that are parts of a continuing process.

$$\text{process}(z^{i-1}, z^i) \Leftrightarrow \big(SO(z^{i-1}, z^i) \vee SO(z^i, z^{i-1})\big) \wedge \max\big(\#S^i(z^{i-1}), \#S^{i-1}(z^i)\big) = 1 \tag{9}$$

Transformations can involve several zones as different UHIs may be engaged. For example, a merge involves a set of zones $Z = \{z_1^{i-1}, \ldots, z_m^{i-1}\} \subset \mathcal{Z}_{i-1}$ and one zone $z^i \in \mathcal{Z}_i$. The zone z^i has to significantly overlap all the zones of Z. On the opposite, no zone of $\mathcal{Z}_{i-1}$ significantly overlaps z^i.

$$\text{merging}(Z, z^i) \Leftrightarrow \big(S^{i-1}(z^i)\big) \wedge \big(\forall z \in \mathcal{Z}_{i-1}, \neg SO(z, z^i)\big) \tag{10}$$

In the case another zone $z_0^{i-1} \in \mathcal{Z}_{i-1}$ significantly overlaps z^i, we have an annexation instead of a merge.

$$\text{annexation}(z_0^{i-1}, Z, z^i) \Leftrightarrow \big(S^{i-1}(z^i)\big) \wedge \big(\forall z \in Z, \neg SO(z, z^i)\big) \wedge SO(z_0^{i-1}, z^i) \tag{11}$$

The other way round, one zone z^{i-1} at t_{i-1} overlapping a set of zones $Z = \{z_1^i, \ldots, z_m^i\} \subset \mathcal{Z}_i$ at t_i corresponds to a split. This requires that z^{i-1} significantly overlaps all the zones of Z while no zone overlaps z^{i-1} significantly.

$$\text{splitting}(z^{i-1}, Z) \Leftrightarrow \big(S^i(z^{i-1})\big) \wedge \big(\forall z \in \mathcal{Z}_i, \neg SO(z, z^{i-1})\big) \tag{12}$$

Instead, a separation occurs if one zone z_0^i significantly overlaps z^{i-1}.

$$\text{separation}(z^{i-1}, Z, z_0^i) \Leftrightarrow \big(S^i(z^{i-1})\big) \wedge \big(\forall z \in Z, \neg SO(z, z^{i-1})\big) \wedge SO(z_0^i, z^{i-1}) \tag{13}$$

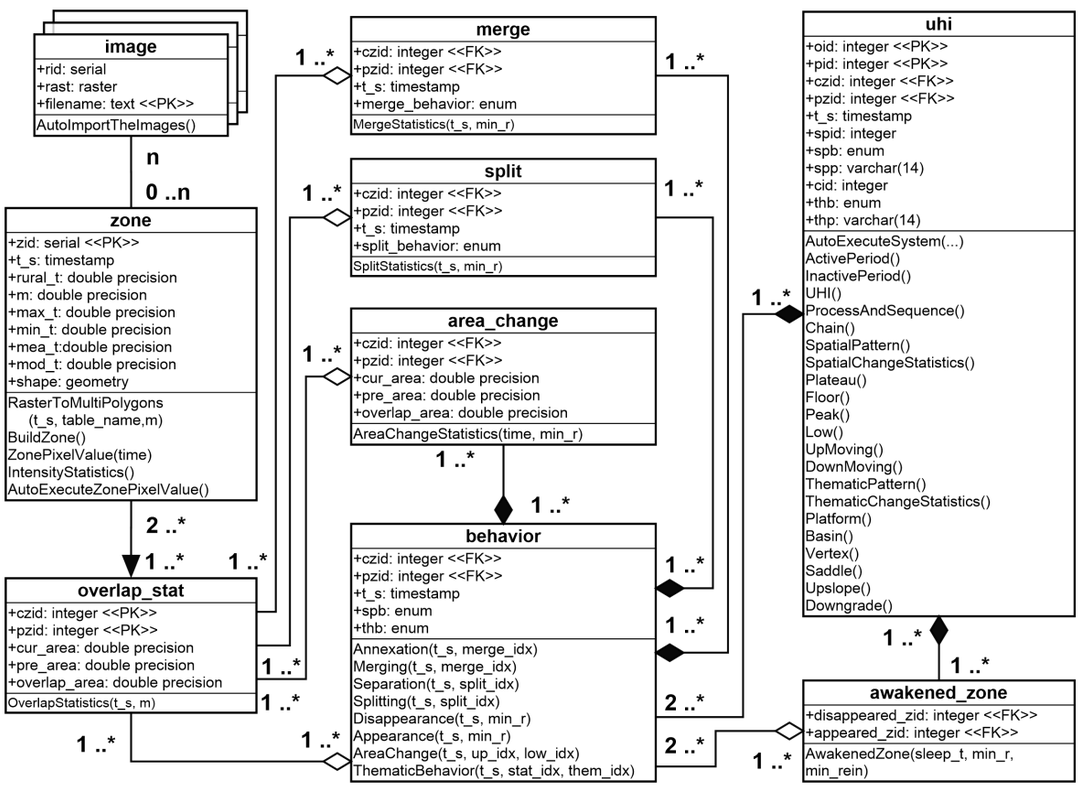

Figure 7: Database tables, functions, and their associations and generations for tracking spatial and thematic behaviors of UHIs over time.

Finally, a zone $z_i \in \mathcal{Z}_i$ can appear or disappear at time t_i. In the first case, it is not related to any zone in $\mathcal{Z}_{i-1}$, in the second case, it is not be related to any zone in $\mathcal{Z}_{i+1}$.

$$\text{appearance}(z^i) \Leftrightarrow \forall z \in \mathcal{Z}_{i-1}, \neg \left(SO(z, z^i) \vee SO(z^i, z)\right) \tag{14}$$

$$\text{disappearance}(z^i) \Leftrightarrow \forall z \in \mathcal{Z}_{i+1}, \neg \left(SO(z, z^i) \vee SO(z^i, z)\right) \tag{15}$$

Zones would have different spatial behaviors when their overlappings are in different scenarios. For example, if $SO(z_b, z_c)$ and $SO(z_b, z_a)$ are determined, it's a merge. With more conditions of $SO(z_b, z_c)$ and $SO(z_a, z_b)$, an annexation would be obtained (Figure 6). We may also have $SO(z_a, z_d)$, which leads to a split. In this case, z_a would have a special behavior, i.e., combining of a splitting and a merging at the same time.

Whenever spatial behavior of the zones (z^{i-1}, z^i) has been determined, UHI represented as a time series of zones $\{z_n^i\}$ $(n = 1, ..., m)$ can be tracked instantly such that thematic changes can be investigated in time series. If s_n^i varies in a limited range and is almost the same as s_n^{i-1}, it is reasonable to consider that thematic behavior of z_n^i is *stationary* computed as in Equation 16. However, it can be depicted as *increasing* or *decreasing* if the relative change exceeds the upper limit or the lower limit.

$$\frac{s_n^i}{s_n^{i-1}} \in [1 - \varepsilon_t', 1 + \varepsilon_t'] \tag{16}$$

4. Empirical evaluation

4.1. System Implementation

The model has been implemented in PostgreSQL 10 to simulate behaviors and track their changes during the complete life-cycles. Figure 7 summaries the classes as discrete records in the tables and represents their associations. First, a time series of temperature images generated from hourly

SQL 1 FUNCTION ActivePeriod()

```
1 INSERT INTO period(pid, t_s, czid, pzid, spb, thb)
2 SELECT max(path) AS path, per.t_s, per.czid, per.pzid, per.spb, per.thb
3 FROM  (WITH RECURSIVE per_u(path, t_s, czid, pzid, spb, thb)
4        AS  (SELECT row_number() OVER (ORDER BY t_s) AS path, root.t_s,
5                    root.czid, root.pzid, root.spb, root.thb
6             FROM   behavior AS root UNION
7             SELECT leaf.path, root.t_s, root.czid, root.pzid, root.spb, root.thb
8             FROM   behavior AS root, per_u AS leaf
9             WHERE  root.czid = leaf.pzid
10            AND    leaf.pzid > 0 AND leaf.spat_beh <> 'separa_d_obj'
11            AND    root.spb <> 'annexa_d_obj'
12            AND    root.spb <> 'merging' AND root.spat_beh <> 'splitting')
13       SELECT * FROM per_u ORDER BY path, t_s) AS per
14 GROUP BY per.t_s, per.czid, per.pzid, per.spb, per.thb;
```

observed air temperatures are stored in a set of `image` tables. Hence, all the zones are extracted from temperature images, and their spatial and thematic information is stored in the `zone` table. For example, each row records that a zone uniquely identified by its ID (`zid`) exists as a single polygon (`shape`) at a time stamp (`t_s`), and temperatures in the `shape` are at least with a magnitude (`m`) higher than the reference rural temperature (`rural_t`). Particularly, four types of the thermal intensities are also summarized (`max_t`, `min_t`, `mea_t`, and `mod_t`). In order to determine filiation relations between zones, overlapping areas (`overlap_area`) between zones in the current time instant (`czid`) and zones in the previous time instant (`pzid`) have to be calculated in advance. To avoid duplicated calculation, zones which have areal changes and topological transformations are classified into three tables (`merge`, `split`, and `area_change`) such that the `behavior` table can be built as the central domain to describe two types of the behaviors (`spb` and `thb`) at each time stamp (`t_s`). Thus, UHIs (`oid`) can be constructed in the `uhi` table, and each one can have one or several periods (`pid`), and each period combines a time serial of spatial behaviors determined by thematic behaviors. Simultaneously, sequence and process descriptions for spatial behaviors (`spid`) and thematic behaviors (`cid`) are obtained, and their corresponding patterns (`spp` and `thp`) are finally revealed.

It is necessary to identify topological relations associated with zones that can create and destroy an active period (SQL 1), and it is also vital to connect active periods that belong to the same UHI by determining awakened zones that trigger new periods (SQL 2). In SQL 1, lines 4-6 generate serial numbers as the candidates of period IDs and determine the first zone behavior (i.e. named as `root`) in the periods. Lines 7-12 build continual zone behaviors that extend from the roots (i.e. named as `leaf`). More specifically, line 9 connects the leaves on the root. Line 10 avoids endless loop computation by ensuring that the appearance and disappearance behaviors are included in the period, and generates new periods when zones are separated as different objects. Hence, lines 11-12 cut off the extension of leaves when zones are destroyed. Lastly, lines 3-13 execute the recursive computation and lines 2-14 select the maximum value of path used as the final period ID. In SQL 2, lines 5-6 and 7-8 respectively list zones having *appearance* as the head and *disappearance* as the tail, where time interval between them is more than two hours but no longer than the maximum awakened time (lines 9-10). Thus, pairs of the heads and tails that satisfy the awakened condition (lines 11-13) are selected as the awakened candidates (lines 2-3). However, several disappeared zones can map to the same appeared zone in the awakened candidates. On the basis of the candidates which have the minimum sleeping time (lines 19-20), zones having the maximum overlapping area are selected (lines 21-22) from the records of awakened candidates (lines 23-25). Finally, zones satisfying all the conditions are inserted into the awakened table (lines 14-27).

SQL 2 FUNCTION AwakenedZone(sleep_t, min_r, min_rein)

```
INSERT INTO awakened_zone(disappeared_zid, appeared_zid)
SELECT tail_seq.zid AS disap_z, head_seq.zid AS reapp_z,
       (head_seq.t_s - tail_seq.t_s) AS dth_t,
        ST_Area(ST_Intersection(head_seq.geom, tail_seq.geom)) AS i_a
FROM  (SELECT zone.* FROM zone, period
        WHERE  spb = 'appearance' AND zone.zid = period.czid) AS head_seq,
       (SELECT zone.* FROM zone, period
        WHERE  spb = 'disappearance' AND zone.zid = period.pzid) AS tail_seq
WHERE  head_seq.t_s - tail_seq.t_s <= sleep_t * 3600 * '1 second'::INTERVAL
AND   head_seq.t_s - tail_seq.t_s >= 2 * 3600 * '1 second'::INTERVAL
AND   ST_Area(ST_Intersection(head_seq.geom, tail_seq.geom))/ST_Area(head_seq.geom) >= min_r
AND   ST_Area(ST_Intersection(head_seq.geom, tail_seq.geom))/ST_Area(tail_seq.geom) >= min_r
AND   ST_Area(ST_Intersection(head_seq.geom, tail_seq.geom))/ST_Area(head_seq.geom) >= min_rein;

INSERT INTO awakened_zone(disappeared_zid, appeared_zid)
SELECT cand.disap_z, cand.reapp_z
FROM   awakened_cand AS cand,
       (SELECT cand.reapp_z, min(cand.dth_t) AS min_dth_t
        FROM   awakened_cand AS cand,
               (SELECT min(dth_t) AS min_dth_t, disap_z
                FROM   awakened_cand GROUP BY disap_z) AS dth_cand,
               (SELECT max(i_a) AS max_i_a, dth_t, disap_z
                FROM   awakened_cand GROUP BY disap_z, dth_t) AS ints_cand
        WHERE dth_cand.min_dth_t = cand.dth_t AND dth_cand.disap_z = cand.disap_z
        AND   ints_cand.max_i_a = cand.i_a AND ints_cand.disap_z = cand.disap_z
        AND   dth_cand.disap_z = ints_cand.disap_z GROUP BY cand.reapp_z) AS uhi_cand
WHERE  cand.reapp_z = uhi_cand.reapp_z
AND    cand.dth_t = uhi_cand.min_dth_t;
```

4.2. Results

4.2.1. Dynamic behaviors of UHIs

Figure 8 presents seven consecutive days of the intensities (i.e. the mean value of temperature differences at each time instant) in five different magnitudes. Intensities (m = 1 °C) lasting almost all the time suggests that m = 1 °C cannot distinguish temperature difference effectively and proves that zones of UHIs should be with m > 1 °C, as what has been suggested in Section 3.1. Over the seven days, intensities for each magnitude increased gradually accompanying the fact that reference rural temperature also increased from 27.6 °C to 29.2 °C. This reveals that air temperatures in urban areas increase faster than that of the reference rural temperature in this time period, suggesting a typical UHI phenomenon during the summer with big sunshine. The figure also shows that intensities having a larger m were more stable with less variation and with shorter *active* period. For example, the highest peak of the intensities occurred in the mid-night on August 5 when m = 2 °C, while the peak was faded when m = 5 °C. This suggests that a small m would help to describe the overall evolutionary trend of UHIs while a large one could be able to find stable heat resources of UHIs.

Based on the above statistics, Figure 9 draws UHIs in three magnitudes and presents behaviors of three UHIs queried from the `uhi` table, with object IDs (the `oid` column) equalling to 15 (m=2 °C), 17 (m=3 °C), and 10091 (m=4 °C). It shows that the UHI having the largest magnitude contracted insignificantly without any topological transformation and the intensity was stationary over the night. Since this UHI was located in the most dense urban area of Guangzhou, it can be explained that buildings were thermal masses that could release heat continuously and stably over the night, which came from the accumulation of solar radiation fluxes during the daytime. Correspondingly, the UHI having a moderate magnitude contracted by separating several parts from its origin continuously and

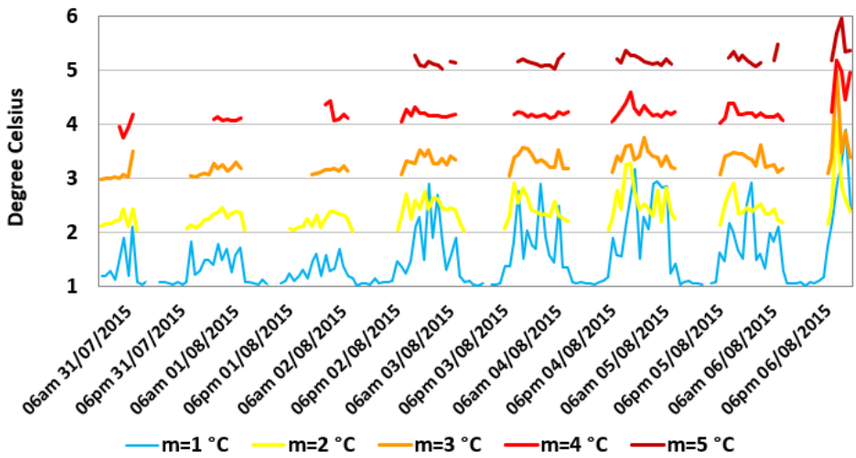

Figure 8: Intensities of UHIs in five different magnitudes for consecutive of seven days.

the intensity decreased gradually. New UHIs occurred from the separation simultaneously. It can be found that temperatures in the less dense urban areas decreased faster than that of the reference rural temperature, leading to the decrease of the intensity and contraction of the zone during the night from 2 am to 4 am. Then, the air started to accumulate heat in the dawn from 5 am to 6 am so that air temperatures increased faster than that of the reference rural temperature, making expansion and merging. Lastly, UHIs contracted and disappeared from the sun rise at 7 am because increase of the reference rural temperature has been faster from then on and temperature differences have been smaller than m=3 °C. In contrast, the UHI having the smallest magnitude expanded gradually before dawn but contracted dramatically in the dawn, and finally disappeared in the early morning. The intensity had a contrary evolutionary trend, which decreased and then increased followed by the other decrease the same corresponding time. Obviously, UHIs in different magnitudes have different evolutions.

Additionally, a UHI can contain several periods (i.e. two active periods are connected by an inactive period in the `pid` column) as presented in Figure 9, meaning that it can either reappear in the next day (for the UHI with `oid`=15) or in several days (for the UHI with `oid`=17). This reveals that UHIs have periodicities and demonstrates that the proposed model can track evolutions of UHIs over longer time compared with previous models, with the establishing of the periodicity.

4.2.2. Thematic evolution of UHIs

To find evolutionary trends of UHIs over seasons, the study investigates changes of UHIs in six weeks covering a continual of six months from July to December in 2015 (Figure 10). It shows that UHIs mostly happened and were the most significant during the night. However, an entire opposite phenomenon is found that UHIs were the most significant at noon on September 30, October 27, and November 25. This abnormal phenomenon always accompanied with a dramatic decrease of the reference rural temperatures that it was sunny in the previous day while it rains in the current day. It can be explained that heat accumulated in the previous day could not disperse immediately during the night because of the thermal insulation contributed by the urban canopy, i.e., rain-rich clouds obstructed the spread of heat. Thus, heat accumulated in the previous day gradually releases in the next day after the rain, and the UHI is getting more obvious contributed by anthropogenic heat fluxes (e.g. heat generated by vehicular flows) in the daytime.

Several findings can also be revealed in Figure 10. In most cases, UHIs with larger magnitudes are more stable with shorter active periods. However, intensities at high-density urban areas (m=4 °C) can vary obviously and reach up to 5.5 °C averagely on September 25 and November 23, making UHIs extremely significant. This phenomenon always accompanied with clear sky in the night followed by

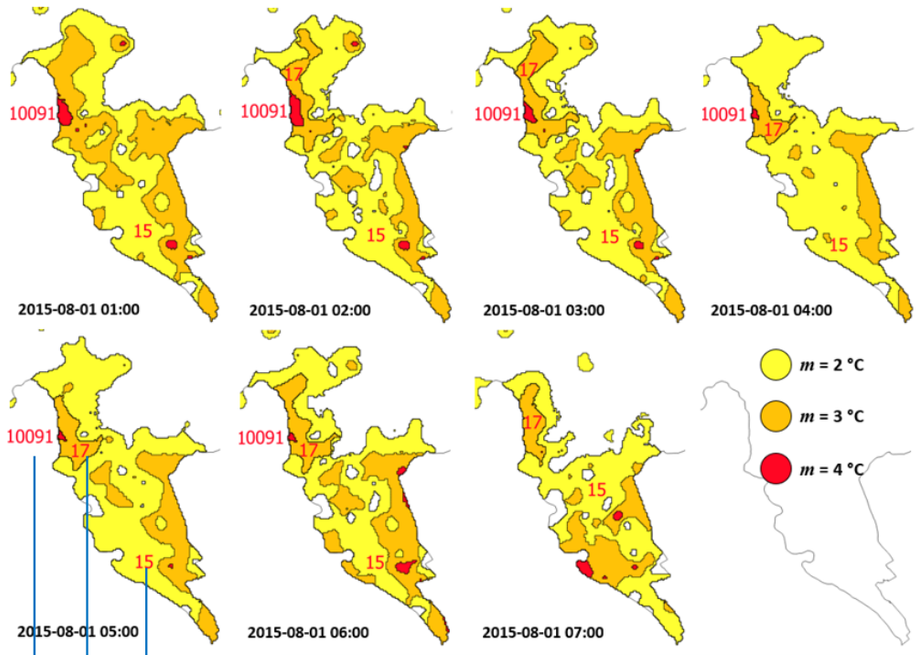

oid	pid	t_s	czid	pzid	spid	spb	spp	cid	thb	thp
15	315	31/7/2015 21:00	512	500	171	annex		159	stationary	
15	315	31/7/2015 22:00	41	512	171	annex		164	decreasing	re_low
15	315	31/7/2015 23:00	56	41	171	annex		186	increasing	le_low
15	315	1/8/2015 0:00	524	56	171	annex		186	increasing	le_low
15	315	1/8/2015 1:00	408	524	249	expan	re_peak	186	increasing	le_low
15	315	1/8/2015 2:00	414	408	250	contr	le_peak	213	decreasing	downgrade
15	315	1/8/2015 3:00	247	414	258	annex		217	stationary	stabilization
15	315	1/8/2015 4:00	533	247	266	contr		221	decreasing	downgrade
15	315	1/8/2015 5:00	537	533	272	annex		227	increasing	re_peak
15	315	1/8/2015 6:00	65	537	272	annex		227	increasing	re_peak
15	315	1/8/2015 7:00	542	65	272	annex		247	decreasing	le_peak
15	315	1/8/2015 8:00	403	542	295	contr		247	decreasing	le_peak
15	315	1/8/2015 9:00	0	403	300	disap		250	null	
15	316	1/8/2015 10:00								
15	316	1/8/2015 22:00								
15	431	1/8/2015 23:00	564	0	346	appea		294	null	
15	431	2/8/2015 0:00	593	564	360	expan		312	increasing	upslope
15	431	2/8/2015 1:00	583	593	360	expan		315	stationary	stabilization
15	431	2/8/2015 2:00	370	583	398	merge		335	increasing	upslope
17	289	1/8/2015 2:00	350	334	178	separ		171	increasing	re_peak
17	289	1/8/2015 3:00	361	350	209	annex		184	decreasing	le_peak
17	289	1/8/2015 4:00	304	361	213	separ		199	stationary	
17	289	1/8/2015 5:00	371	304	241	expan		199	stationary	
17	289	1/8/2015 6:00	384	371	254	annex		216	decreasing	
17	289	1/8/2015 7:00	387	384	272	contr		216	decreasing	
17	289	1/8/2015 8:00	0	387	283	disap		243	null	
17	290	1/8/2015 9:00								
17	290	6/8/2015 17:00								
17	1288	6/8/2015 18:00	627	0	1217	appea		1104	null	
17	1288	6/8/2015 19:00	826	627	1229	merge		1110	increasing	
10091	91	1/8/2015 1:00	112	0	55	appea		30	null	
10091	91	1/8/2015 2:00	121	112	64	annex		35	stationary	
10091	91	1/8/2015 3:00	71	121	67	contr	re_low	35	stationary	
10091	91	1/8/2015 4:00	72	71	67	contr	re_low	35	stationary	
10091	91	1/8/2015 5:00	74	72	67	contr	re_low	35	stationary	
10091	91	1/8/2015 6:00	80	74	84	expan	le_low	35	stationary	
10091	91	1/8/2015 7:00	0	80	90	disap		61	null	

Figure 9: Behaviors of UHIs in three magnitudes of 2, 3, and 4 degrees Celsius.

big sunshine in the morning. This suggests that continuous of clear sky would be likely to generate significant UHIs. It can be explained that both urban and rural areas can release great amount of the heat at high speed of rate in the night with clear sky so that air temperatures in urban areas can increase much faster in the morning even though reference rural temperatures also have dramatic increase. Oppositely, UHIs were insignificant and even could not happen when amplitudes of the reference rural temperatures became much smaller between December 20 and December 23, caused by thick fogs all over the days. A similar phenomenon occurred between August 28 and September 3 that UHIs were short and insignificant over the whole week. However, the mechanism is different, which was because that the heat was dispersed by a rainstorm lasting for the whole week and clouds obstructed absorption of solar radiation fluxes in land surface.

Moreover, continuous of raining (e.g. days between August 28 and September 03) and fogs (e.g. days between December 20 and December 23) could obstruct occurrence of UHIs. Apartment from these weathers, daily occurrence and intensities of UHIs were almost the same from summer to winter, disregarding with different seasons. This new finding may be against the potential perception of the people.

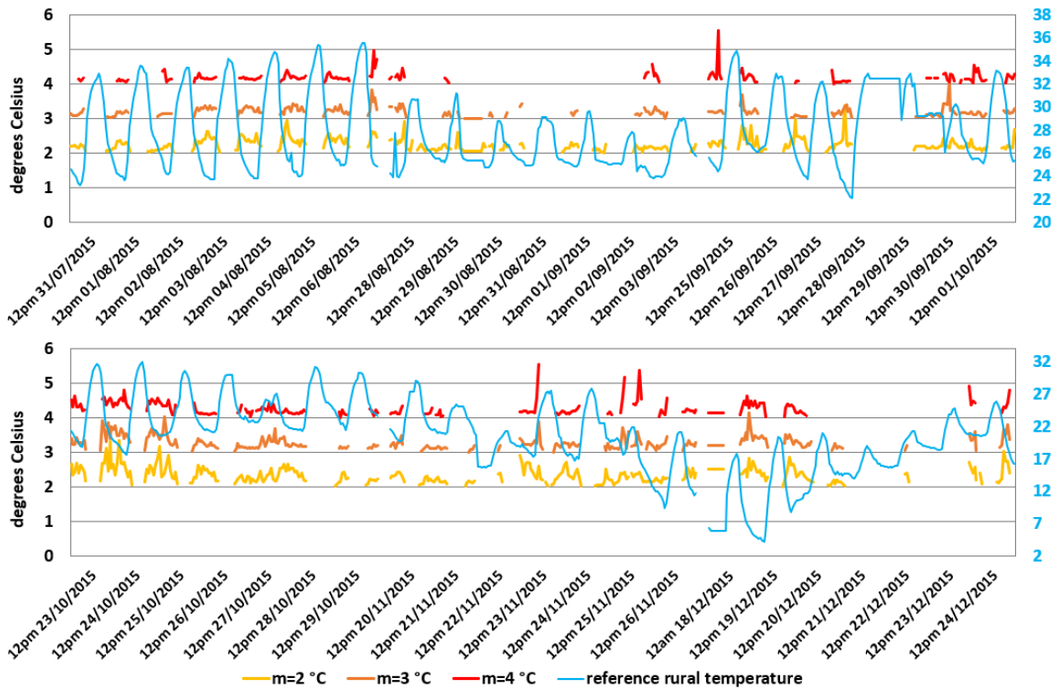

Figure 10: Intensities in three magnitudes over six weeks together with the reference rural temperatures.

4.2.3. Relationship of UHIs in different magnitudes

According to the proposed UHI definition, a UHI in a small magnitude would be more likely to occur with a large zone, so that zones with a large magnitude can locate in the same zone with a small magnitude. Based on the evidence that small and high-density urban areas can accumulate great amount of the heat coming from natural heat fluxes and anthropogenic heat fluxes (Nichol *et al.*, 2009; Zhu *et al.*, 2017), it has reasons to believe that high-density urban areas could be the largest heat resource in a city. Thus, correlation analysis between areas of zones in the same time instant but in different magnitudes would help to explore relationship of UHIs in different magnitudes.

Total areas of UHIs in three magnitudes (m=2, 3, 4 °C) were computed through SQL queries and then correlations of the total areas between m=3, 4 °C (Figure 11) and between m=2, 4 °C (Figure 12) were computed respectively by using R^2. Overall, R^2=0.78 for m=3, 4 °C and R^2=0.59 for m=2, 4 °C for the total six weeks, both of which show positive correlations. The two figures also present that total areas of UHIs were several times (for m=3 °C) to dozens of times (for m=2 °C) larger than that in a large magnitude (m=4 °C).

Particularly, all the values of R^2 for m=3, 4 °C were larger than 0.80 expect for the seven days between September 25 and October 01 (Figure 11), which show strong and positive correlations. Two reasons can be discussed. First, high-density urban areas determined evolution of UHIs in m=4 °C, since the urban areas and zones of the UHIs had significant overlapping most of time. Second, great amount of the heat generated in small and high-density urban areas could diffuse to large and low-density urban areas through air thermal diffusion. This process fundamentally influenced thermal distribution in low-density urban areas and thus made merging and annexation between zones, as what has been obtained and presented in Figure 9. This reasoning can explain why strong and positive correlations could be obtained between areas of zones. Therefore, UHIs in a large magnitude (m=4 °C) could overwhelmingly influence evolution of UHIs in a small magnitude (m=3 °C). Additionally, the influence could cross different seasons because $R^2 \geqslant$0.80 maintained from August to December basically. There was a weak and positive correlation (R^2=0.43) between September 25 and October 01. Given the fact that the weather was changing continuously during these days, i.e., fogs, clouds, and sunshine were mixed without rules, it can be reasoned that unstable weather can impede heat absorption and thermal diffusion notably, leading to the disappearance of UHIs.

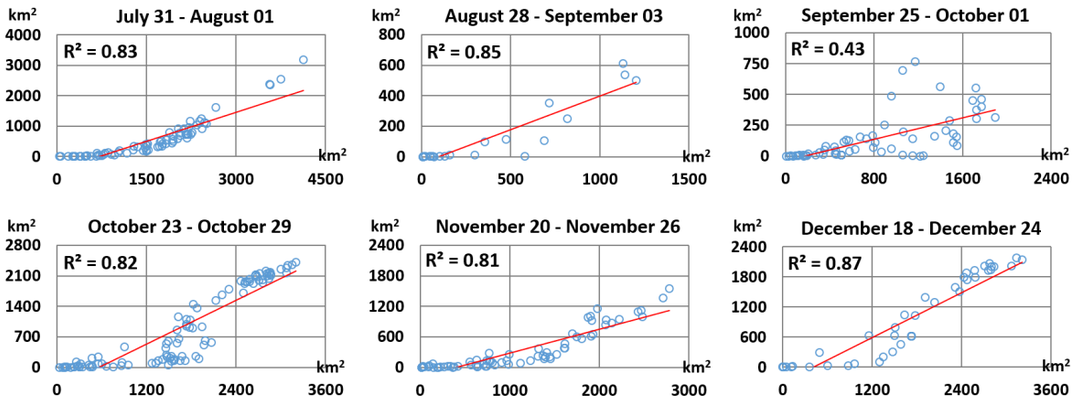

Figure 11: Correlation analysis between areas of UHIs in m=3 °C (x axis) and m=4 °C (y axis) over six weeks.

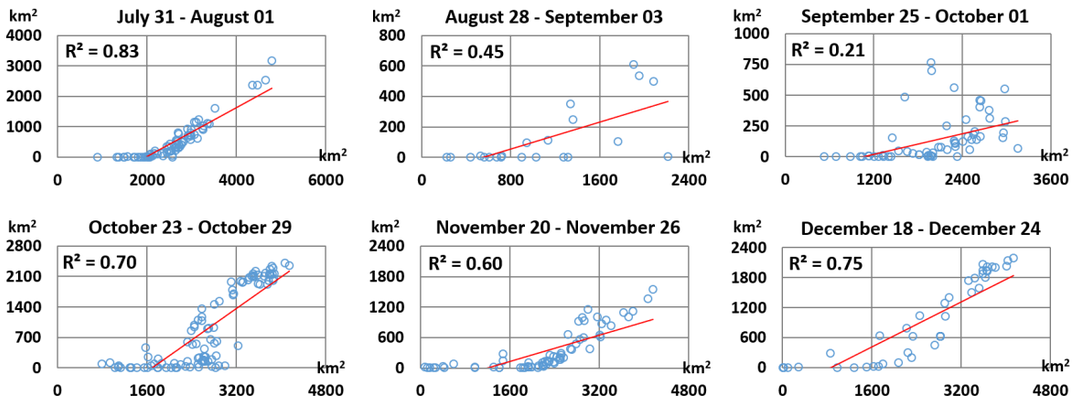

Figure 12: Correlation analysis between areas of UHIs in m=2 °C (x axis) and m=4 °C (y axis) over six weeks.

Even though all the values of R^2 for m=2,4 °C (Figure 12) were smaller than that for m=3,4 °C (Figure 11), all of them obtained positive correlation. Surprisingly, strong and positive correlations still remained ($R^2 \geqslant 0.70$) between July 31 and August 01, October 23 and October 29, and December 18 and December 24 for UHIs in m=2,4 °C. It can be explained that heat from small and high-density urban areas still had capacity to influence evolution of UHIs, reaching up to much larger areas partly containing urban-and-rural mixed regions.

5. Discussion and Conclusion

This study established an object-oriented data model organized by five hierarchical graphs that allows tracking of thematic and spatial behaviors of UHIs with several periods. Instead of focusing on absolute air temperatures of UHIs, this study proposed the concept of *intensity* as the statistics of temperature differences between urban temperatures and reference rural temperatures to model different behaviors. Each UHI also has a *magnitude* to maintain its significance so that various phenomena can be explored in different magnitudes. Empirical evaluation based on a well designed and implemented database management system suggests that the proposed model can process a large set of images automatically (e.g. images covering a whole year) and allow queries to explore evolutions and characteristics of UHIs effectively.

Four important findings in this study can be summarized. First, clear sky in the night connecting big sunshine in the next morning would easily promote extremely high intensities of UHIs. Second, UHIs in a particular magnitude could maintain their intensities and daily duration not only in summer but also across seasons to winter when without disturbing of rain and fog weathers. Third, UHIs normally occur in the night over seasons, while they can also be very significant at noon because of a sunny-to-raining weather in a continuous of two days. Lastly, UHIs in a larger magnitude are more locationally associated with smaller spatial extents and shorter duration of active periods. Small

and high-density urban areas could be the most largest heat resource and create UHIs in the largest magnitude that fundamentally determines and influences evolution of UHIs in smaller magnitudes, covering lager urban areas.

In the model, a UHI has either topological transformation or areal change at each time instant. While, an active object shall have explicit spatial and thematic properties all the time such that correlations between areas and temperatures for UHIs can be determined at each time instant. In this consideration, the model can be refined in the future that each object has areal changes and thematic changes continuously and possibly associated with the topological transformations at a time instant.

The model can be used not only for tracking of UHIs but also for other environmental phenomena when they can be modelled as field objects appropriately. For example, hurricanes and water pollutions can be viewed as fields as well with various intensities in their spatial extents, evolution of which can be tracked continuously by using obtained remote sensing images; while, further development of the model is needed to enable locational tracking since these phenomena can be typical moving objects that can move far away from their origins significantly.

References

Bothwell, J., Yuan, M., 2010. Apply concepts of fluid kinematics to represent continuous space–time fields in temporal GIS. *Annals of GIS*, 16(1), 27–41.

Bothwell, J., Yuan, M., 2011. A Kinematics-based GIS Methodology to Represent and Analyze Spatiotemporal Patterns of Precipitation Change in IPCC A2 Scenario. *ACM SIGSPATIAL GIS '11*, 152–161.

Bothwell, J., Yuan, M., 2012. A Spatiotemporal GIS Framework Applied to the Analysis of Changes in Temperature Patterns. *Transactions in GIS*, 16(6), 901–919.

Buyantuyev, A., Wu, J., 2010. Urban heat islands and landscape heterogeneity: linking spatiotemporal variations in surface temperatures to land-cover and socioeconomic patterns. *Landscape Ecology*, 25(1), 17–33.

Claramunt C., Thériault M., 1995. Managing Time in GIS: An Event-Oriented Approach. *Proceedings of the International Workshop on Temporal Databases: Recent Advances in Temporal Databases*, 23–42.

Cohn, E. G., Rotton, J., 2000. Weather, seasonal trends and property crimes in Minneapolis, 1987-1988. A moderator-variable time-series analysis of routine activities. *Journal of Environmental Psychology*, 20(3), 257–272.

Chai, H. X., Cheng, W. M., Zhou, C. Q., Chen, X., Ma, X. Y., Zhao, S. M., 2011. Analysis and comparison of spatial interpolation methods for temperature data in Xinjiang Uygur Autonomous Region, China. *Natural Science*, 3(12), 999–1010.

Del Mondo, G., Rodríguez, M. A., Claramunt, C., Bravo, L., Thibaud, R., 2013. Modelling Consistency of Spatio-temporal Graphs, *Data & Knowledge Engineering, Elsevier*, 84(1), 59–80.

Ding, Z., Guo, P., Xie, F., et al, 2015. Impact of diurnal temperature range on mortality in a high plateau area in southwest China: A time series analysis. *Science of the Total Environment*, 526, 358–365.

Field, S., 1992. The effect of temperature on crime. *British Journal of Criminology*, 32(3), 340–351.

Fung, W. Y., Lam, K. S., Hung, W. T., Pang, S. W., Lee, Y. L., 2006. Impact of urban temperature on energy consumption of Hong Kong. *Energy*, 31(14), 2623–2637.

Goodchild M. F., Yuan M. and Cova T. J. 2007. Towards a general theory of geographic representation in GIS. *International Journal of Geographical Information Science*, 21(3), 239–260.

Hornsby K., Egenhofer M. J., 2000. Identity-based change: a foundation for spatio-temporal knowledge representation. *International Journal of Geographical Information Science*, 14(3), 207–224.

Hornsby, K. S., Cole, S., 2007. Modeling Moving Geospatial Objects from an Event-based Perspective. *Transactions in GIS*, 11(4), 555–573.

Hofstra, N., Haylock, M., New M., Jones, P., Frei, C., 2008. Comparison of six methods for the interpolation of daily, European climate data. *Journal of Geographical Research*, 113, D21110. doi:10.1029/2008JD010100

Hu. L., Brunsell, N. A., 2015. A new perspective to assess the urban heat island through remotely sensed atmospheric profiles. *Remote Sensing of Environment*, 158, 393–406.

Irmak, A., Ranade, P. K., Marx, D., Irmak, S., Hubbard, K. G., Meyer, G. E., Martin, D. L., 2010. Spatial Interpolation of climate variables in Nebraska. *Transactions of the ASABE*, 53(6), 1759–1771.

Keramitsoglou, I., Kiranoudis, C. T., Ceriola, G., Weng, Q., Rajasekar, U., 2011. Identification and analysis of urban surface temperature patterns in Greater Athens, Greece, using MODIS imagery. *Remote Sensing of Environment*, 115(12), 3080–3090.

Kenney, W. L., Craighead, D. H., Alexander, L. M., 2014. Heat Waves, Aging, and Human Cardiovascular Health. *Medicine & Science in Sports & Exercise*, 46(10), 1891–1899.

Kourtidis, K., Georgoulias, A. K., Rapsomanikis, S., Amiridis, V., Keramitsoglou, I., Hooyberghs, H., Maiheu, B., Melas, D., 2015. A study of the hourly variability of the urban heat island effect in the Greater Athens Area during summer. *Science of the Total Environment*, 517, 162–177.

Li, J., Liang, Y., and Wan, J., 2013. Geo-Ontology-Based Object-Oriented Spatiotemporal Data Modeling. *Lecture Notes in Computer Science*, 7719, 302–317.

McIntosh, J., Yuan, M., 2005. Assessing Similarity of Geographic Processes and Events. *Transactions in GIS*, 9(2), 223–245.

Morabito, M., Crisci, A., Moriondo, M., 2012. Air temperature-related human health outcomes: Current impact and estimations of future risks in Central Italy. *Science of the Total Environment*, 441, 28–40.

Nichol, J. E., Fung, W. Y., Lam K. S., Wong, M. S., 2009. Urban heat island diagnosis using ASTER satellite images and 'in situ' air temperature. *Atmospheric Research*, 94(2), 276–284.

Nixon, V., Hornsby, K. S., 2010. Using geolifespans to model dynamic geographic domains. *International Journal of Geographical Information Science*, 24(9), 1289–1308.

Pultar, E., Cova, T. J., Yuan, M., Goodchild, M .F., 2010. EDGIS: a dynamic GIS based on space time points. *International Journal of Geographical Information Science*, 24(3), 329–346.

Papakostas, K., Mavromatis, T., Kyriakis, N., 2010. Impact of the ambient temperature rise on the energy consumption for heating and cooling in residential buildings of Greece. *Renewable Energy*, 35(7), 1376–1379.

Renolen, A., 2000. Modelling the Real World: Conceptual Modelling in Spatiotemporal Information System Design. *Transactions in GIS*, 4(1), 23–42.

Rotton, J., Cohn, E. G., 2004. Outdoor temperature, climate control, and criminal assault. *Environment and Behaivor*, 36(2), 276–306.

Stahl, K., Moore, R. D., Floyer, J. A., Asplin, M. G., McKendry, I. G., 2006. Comparison of approaches for spatial interpolation of daily air temperature in a large region with complex topography and highly variable station density. *Agricultural and Forest Meteorology*, 139, 224–236.

Toparlar, Y., Blocken, B., Vos, P., Heijst, G. J. F., Janssen, W. D., Hooff, T., Montazeri, H., immermans, H. J. P., 2015. CFD simulation and validation of urban microclimate: A case study for Bergpolder Zuid, Rotterdam. *Building and Environment*, 83, 79–90.

Wong, M. S., Nichol, J. E., 2013. Spatial variability of frontal area index and its relationship with urban heat island intensity. *International Journal of Remote Sensing*, 34(3), 885–896.

Wong, M. S., Zhu, R., Liu, Z., Lu, L., Peng, J., Tang, Z., Lo, C. H., Chan, W. K., 2016. Estimation of Hong Kong's solar energy potential using GIS and remote sensing technologies. Renewable Energy, 99, 325–335.

Wu, F., Wang, X., Cai, Y., Yang, Z., Li, C., 2012. Spatiotemporal analysis of temperature-variation patterns under climate change in the upper reach of Mekong River basin. *Science of the Total Environment*, 427-428, 208–218.

Yuan, M., Hornsby, K., 2008. *Computation and Visualization for Understanding Dynamics in Geographic Domains*. CRC Press.

Yuan, C., Ng. E., 2012. Building porosity for better urban ventilation in high-density cities - A computational parametric study. *Building and Environment*, 50, 176–189.

Zhou, B., Kropp, J., Rybski, D., 2016. Assessing Seasonality in the Surface Urban Heat Island of London. *Journal of Applied Meteorology and Climatology*, 55, 493–505.

Zhu, R., Guilbert, E., Wong, M.S., 2016. Object-oriented tracking of the dynamic behavior of urban heat islands. *International Journal of Geographical Information Science*, 31(2), 405–424.

Zhu, R., Wong, M. S., Guilbert, E., Chan, P. W., 2017. Understanding heat patterns produced by vehicular flows in urban areas. *Scientific Reports*, 7, 16309.